Filtration of Highly Compactible Filter Cake: Variable Internal Flow Rate

D. J. Lee and S. P. Ju
Dept. of Chemical Engineering, National Taiwan University, Taipei, Taiwan 10617

J. H. Kwon
Dept. of Environmental Science, Inje University, Obang-dong, Kimhae, Korea 621-749

F. M. Tiller
Dept. of Chemical Engineering, University of Houston, Houston, TX 77204

Conventional analyses used to interpret filtration data assume a constant internal liquid flow rate (q_L) and a negligible solid velocity (the constant-q_L approximation). To interpret such data, the upper bounds of errors to estimate α_{av} and k_{av} were analytically derived by the constant-q_L approximation. The solution of the filtration model that incorporates a nonzero solid velocity was then analytically derived. When filtering a highly compactible filter cake, the cake was first compacted toward the filter medium that forms a skin layer and, in doing so, rapidly reaches the steady-state distribution predicted by the constant-q_L approximation. Except at the first stage of the filtration, the approach of Tiller et al. (1999) is valid for interpreting filtration data of a highly compactible filter cake. Furthermore, the constant-q_L approximation provides the upper limit of errors in terms of estimating cake characteristics regardless of the solid velocity effect.

Introduction

The conventional filtration/consolidation theory originates from Ruth's pioneering works (Ruth et al., 1933a,b; Ruth, 1935, 1946), in which a two-resistance theory was proposed by using an electric analogy. According to that theory, the total resistance in filtration comprises a series of resistances of a medium and that of a cake. Tiller, and Shirato and coworkers developed the contemporary two-resistance theory on the basis of compressible cake filtration. Wakeman (1981a,b) reviewed the pertinent literature prior to 1981. Recently, He et al. (1997a,b) reviewed related investigations on filter-cake characteristics.

The conventional filtration/consolidation theory consists of two steps: (1) combining the mass-balance equation and the momentum-balance equation (Darcy's law) for liquid phase in the cake to form the governing equation with both porosity and liquid pressure as dependent variables, and (2) assuming that only point contacts exist between particles. With the assistance of some empirical equations related to solid pressure and porosity, the number of dependent variables in the differential equation obtained from step 1 reduces to only one, normally representing the solid pressure. Under appropriate initial/boundary conditions, the governing equations can be analytically or numerically solved. Models in the earlier literature differ in terms of the different constitutive equations and boundary/initial conditions used.

Prediction of filter performance can be based on pure experiment or on theory combined with experiment. Improved theory and understanding of the basic phenomena lead to models that can be used with more confidence. Most filtration theories assumed that the solids in the filter cake are not in motion, or equivalently, the superficial flow rate of liquid (q_L) is independent of distance x (Tiller, 1966). However, several investigations stated that the internal liquid flow rate should vary with the distance, particularly when dealing with a highly compactible filter cake (Shirato et al., 1969, 1970; Wakeman, 1978; Sorensen and Hansen, 1993). Failure to understand the underlying theory of flow through compactible cakes has been the source of many industrial failures. Understanding the theory of variable flow rate is fundamental to understanding the movement and compaction of the solid

Correspondence concerning this article should be addressed to D. J. Lee.

phase in a cake. Individuals who comprehend the significance of the variable superficial flow rate will have improved familiarity with compactible cake behavior.

Tiller and Copper (1960) appear to be the first to cover the q_L-variation. [*Note:* There is a significant error in Tiller and Copper's derivation, which has been corrected in an erratum attached to Tiller and Shirato (1964).] Tiller and Huang (1961) provided the second discussion on the variation of q_L. Recently, Cleveland et al. (1996) and Sorensen and coworkers (Sorensen and Hansen, 1993; Sorensen et al., 1995, 1996a,b; Sorensen and Sorensen, 1997a,b) discussed filtration of materials with extremely high compressibility. According to their results, compressive pressure would not affect the filtration rate. Tiller and Kwon (1998) discussed the so-called "unexpected behavior" of a highly compactible sludge cake. Tiller et al. (1999) examined the q_L profile in a highly compactible filter cake. As expected, their findings reveal that the more compactible the cake implies a larger deviation for the internal flow rate from the constant-q_L approximation. However, Tiller et al. (1999) did not address the possible errors incurred when estimating the cake characteristics on the basis of the constant-q_L approximation. Furthermore, their approximate solution for q_L-variation is derived on the basis of the formula on the constant-q_L assumption. Despite the somewhat controversial nature of such a treatment, its validity has never been satisfactorily examined. Therefore, in this work, we analytically elucidate these two issues.

Model of Cake Filtration

Figure 1 depicts the one-dimensional filtration process. The domain under consideration encompasses the entire cake body, where $x=0$ denotes the filter medium and $x=L$ represents the cake surface.

Darcy's law interprets the pressure drop in a porous medium, which is strictly valid in an isotropic, stationary porous matrix (Jonsson and Jonssen, 1992a,b). Shirato et al. (1969, 1970) introduced a relative velocity term into the Darcy equation, leading to the so-called "Darcy-Shirato model" as follows:

$$\frac{dP_L}{dx} = \frac{\mu \epsilon_L}{k}(u_L - u_s) \tag{1a}$$

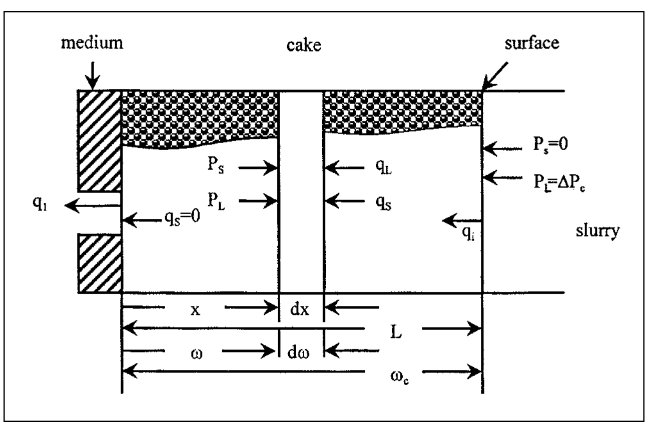

Figure 1. Filter cake.

on the basis of spatial coordinate, or

$$\frac{dP_L}{d\omega} = \mu \alpha \epsilon_L (u_L - u_S) \tag{1b}$$

on the basis of material coordinate. In Eqs. 1a and 1b, P_L is the liquid pressure; ϵ_L the porosity; k the permeability; α, the local specific resistance of cake; μ, the liquid viscosity; and u_L and u_S are the liquid velocity and the solid velocity, respectively. The spatial coordinate and material coordinate are related by $d\omega = (1-\epsilon_L)dx$.

Assume that the gravity force and inertial terms can be neglected and that the solid particles are not deformable. Also assume that only point contacts exist between particles. Then, at a fixed time, the change in liquid pressure gradient equals the negative change in a solid pressure gradient:

$$\frac{\partial P_L}{\partial x} = -\frac{\partial P_S}{\partial x}, \tag{2}$$

where P_S denotes the compressive pressure.

The mass balance of liquid phase can be formulated as the rate of flow q_L in at x minus the rate of flow q_I out at $x=0$ equals the rate of change of liquid in distance x. That is,

$$q_L(x,t) - q_\mathrm{I}(t) = \frac{\partial}{\partial t}\int_0^x \epsilon_L(x,t)\,dx, \tag{3}$$

where q_I is the flow rate of filtrate. By considering the no-flux boundary condition at the exit, a similar formulation can be stated for the solid phase as follows:

$$q_S(x,t) = \frac{\partial}{\partial t}\int_0^x \epsilon_s(x,t)\,dx, \tag{4}$$

where ϵ_s denotes the solidosity $(=1-\epsilon_L)$. While assuming that ϵ_L is a smooth function of time and space, differential Eqs. 3 and 4 yields

$$\left(\frac{\partial q_L}{\partial x}\right)_t = \left(\frac{\partial \epsilon_L}{\partial t}\right)_x \tag{5}$$

and

$$\left(\frac{\partial q_S}{\partial x}\right)_t = \left(\frac{\partial \epsilon_S}{\partial t}\right)_x. \tag{6}$$

Since $\epsilon_L + \epsilon_s = 1$ by definition, Eqs. 5 and 6 can be combined into the following continuity equation in differential form:

$$\left(\frac{\partial q_L}{\partial x}\right) + \left(\frac{\partial q_s}{\partial x}\right) = 0. \tag{7}$$

The preceding equations, together with the definitions $q_L = \epsilon_L u_L$, $q_s = (1-\epsilon_L)u_s$, lead to the following equation:

$$q_L = -\frac{(1-\epsilon_L)k}{\mu}\left(\frac{\partial P_S}{\partial x}\right)_t + \epsilon_L q_\mathrm{I}. \tag{8}$$

While assuming that ϵ_L is a function of P_s only, differentiating Eq. 8 with respect to x and substituting into Eq. 5 yields

$$\frac{\partial}{\partial x}\left(\frac{k\epsilon_s}{\mu}\frac{\partial P_s}{\partial x}\right)+q_1\frac{d\epsilon_s}{dP_s}\left(\frac{\partial P_s}{\partial x}\right)-\frac{d\epsilon_s}{dP_s}\left(\frac{\partial P_s}{\partial t}\right)=0. \quad (9)$$

Equation 9 is the governing equation for P_s on the basis of Darcy-Shirato model. Tiller et al. (1999) discussed the other forms of governing equations in relation to different models of relative velocity.

Constitutive equations for k and ϵ_s as functions of P_s are necessary to complete the formulation. Most related works have adopted the following power-law-type constitutive equations:

$$\left(\frac{\alpha}{\alpha_0}\right)^{1/n}=\left(\frac{k}{k_0}\right)^{-1/\delta}=\left(\frac{\epsilon_s}{\epsilon_{s0}}\right)^{1/\beta}=a+bP_s, \quad (10)$$

where a can be 0 or 1 (Tiller, 1953, 1955, 1958; Tiller and Cooper, 1960, 1962; Tiller and Shirato, 1964; Tiller and Green, 1973; Tiller and Yeh, 1985, 1987; Tiller et al., 1995; Lu et al., 1970; Wakeman et al., 1991; Stamatakis and Tien, 1991; Matsuda et al., 1994). Notably, earlier studies frequently assumed that $a=0$ and $b=P_{\mathrm{ref}}^{-1}$, where P_{ref} is a reference pressure. Such a set of constitutive equations has its limitations at $P_s\to 0$ limit. Consequently, most recent works accept the following parameter set: $a=1$ and $b=P_a^{-1}$, where P_a denotes the threshold pressure above which the cake could largely deform (Leu, 1986).

With the constitutive equations defined in Eq. 10, Eq. 9 can be rearranged into the following dimensionless form:

$$\frac{\partial}{\partial X}\left((1+\gamma P)^{\beta-\delta}\frac{\partial P}{\partial X}\right)+Q^*(1+\gamma P)^{\beta-1}\left(\frac{\partial P}{\partial X}\right)-Q^*(1+\gamma P)^{\beta-1}\left(\frac{\partial P}{\partial \tau}\right)=0. \quad (11)$$

The dimensionless variables in Eq. 11 are defined as follows: $P=P_s/\Delta P_c$, $\gamma=\Delta P_c/P_a$ (usually large), $Q^*=q_1/(P_a k_0/\beta L\mu)=T/t_q$, $\tau=t/t_q$, and $X=x/L$, where $T=\beta L^2\mu/P_a k_0$ and $t_q=L/q_1$, with the latter denoting the characteristic time for the filtrate to flow through the cake.

If the P_s-variation across the cake can be properly solved according to Eq. 11, then the average characteristics of a filter cake can be estimated.

Internal Flow Rate and Average Cake Characteristics

On the basis of the Darcy-Shirato equation, the relative flow rate can be defined as follows:

$$q_R=\epsilon_L(u_L-u_S)=\frac{k}{\mu}\frac{dP_L}{dx}=\frac{1}{\mu\alpha}\frac{dP_L}{d\omega}. \quad (12)$$

The average specific resistance α_{av} and average permeability k_{av} are defined as follows:

$$\alpha_{\mathrm{av}}=\frac{\Delta P_c}{\int_0^{\omega_c}\mu q_R\,d\omega} \quad (13a)$$

and

$$k_{\mathrm{av}}=\frac{\int_0^L \mu q_R\,dx}{\Delta P_c}. \quad (13b)$$

While assuming no q_L variation occurs along the cake thickness, that is, $q_R=q_L=q_1$, then Eqs. 13a and 13b can be integrated explicitly as follows:

$$\alpha_{\mathrm{av}}^C=\frac{\Delta P_c}{\mu q_1\omega_c} \quad (14a)$$

and

$$k_{\mathrm{av}}^C=\frac{\mu q_1 L}{\Delta P_c}. \quad (14b)$$

The superscript C in Eqs. 14a and 14b denotes "constant-q_L" assumption, which is generally adopted in conventional analysis. With the definitions of $\bar{q}_{R,\omega}=(1/\omega_c)\int_0^{\omega_c}q_R\,d\omega$ and $\bar{q}_{R,x}=(1/L)\int_0^L q_R\,dx$, Eqs. 13a and 13b can be rearranged as follows:

$$\alpha_{\mathrm{av}}=\frac{\Delta P_c}{\mu\bar{q}_{R,\omega}\omega_c} \quad (15a)$$

and

$$k_{\mathrm{av}}=\frac{\mu\bar{q}_{R,x}L}{\Delta P_c}. \quad (15b)$$

As a result, according to Eqs. 14 and 15, the ratio of the estimated properties are as follows:

$$F_\omega=\frac{\bar{q}_{R,\omega}}{q_1}=\frac{\alpha_{\mathrm{av}}^c}{\alpha_{\mathrm{av}}} \quad (16a)$$

and

$$F_x=\frac{q_1}{\bar{q}_{R,x}}=\frac{k_{\mathrm{av}}^c}{k_{\mathrm{av}}}. \quad (16b)$$

Notably, since both $\bar{q}_{R,\omega}$ and $\bar{q}_{R,x}$ are less than q_1, $\alpha_{\mathrm{av}}^c<\alpha_{\mathrm{av}}$ ($F_\omega<1$) and $k_{\mathrm{av}}^c>k_{\mathrm{av}}$ ($F_x>1$).

Based on the constant-q_L assumption, the farther the F_ω value deviates from unity implies a larger error in estimating α_{av} or k_{av}. However, evaluating $\bar{q}_{R,\omega}$ and $\bar{q}_{R,x}$ requires *a priori* knowledge of variation in q_L. More comprehensive results could be obtained by numerically solving Eq. 11, which is highly nonlinear, particularly for a highly compactible filter cake. For a highly compactible filter cake, Tiller et al. (1999) revealed that although the change in q_L across the cake is mild, the change in q_R could be significant. Such an occurrence can lead to a significant error in estimating α_{av} or k_{av}.

Quantitatively estimating F_ω and F_x values requires knowledge regarding the variation of q_R across the cake. The fluid flow field in the filter cake was generally assumed to reach a pseudo-steady state during filtration. Except for the very beginning of filtration, Eq. 11 can be approximated by the following pseudo-steady-state equation:

$$\frac{d}{dX}\left((1+\gamma P)^{\beta-\delta}\frac{dP}{dX}\right)+Q^{*}(1+\gamma P)^{\beta-1}\left(\frac{dP}{dX}\right)=0. \quad (17)$$

If further assuming that $u_s = 0$ ($q_L = q_1$), with the assistance of Eq. 8, Eq. 17 could be reduced to

$$\frac{d}{dX}\left((1+\gamma P)^{-\delta}\frac{dP}{dX}\right)=0, \quad (18)$$

which is the case for an incompressible cake. Herein, we denote Eq. 18 as the "zero-u_s" case; meanwhile, Eq. 17 is denoted as the "nonzero-u_s" case.

Zero-u_s Case

Starting from the conventional filtration theory by assuming a constant-q_L, Tiller et al. (1999) derived the following expression for q_L-variation:

$$\frac{\left[\frac{\epsilon_{s\,av}}{\phi_S}-1\right]}{\epsilon_{s0}}\left[1-\frac{q_L}{q_1}\right]=\frac{1}{C}\left[\frac{1-\delta}{1-n}\right]\left\{\left(1+\frac{\Delta P_c}{P_a}\right)^{1-n}-\left[C\left(1-\frac{x}{L}\right)+1\right]^{(1-n)/(1-\delta)}\right\}-\frac{x}{L}\left[C\left(1-\frac{x}{L}\right)+1\right]^{\beta/(1-\delta)}, \quad (19)$$

where $C=(1+(\Delta P_c/P_a))^{1-\delta}-1$. At the cake's surface, where $x = L$, Eq. 19 reaches its maximum value, indicating that the upper bound of q_L-variation is as follows:

$$\frac{q_i}{q_1}=1-\left[\frac{\epsilon_{s\,av}-\epsilon_{s0}}{\epsilon_{s\,av}-\phi_s}\right]\phi_s. \quad (20)$$

Notably, ϵ_{s0} is generally less than 0.05 for a highly compactible filter cake. Therefore, Eq. 20 states that the maximum variation of q_L/q_1 is limited to 0.05 (Tiller et al., 1999).

Using the definition of q_R, Eq. 12, and Eq. 19 leads to the following expression:

$$\frac{q_R}{q_1}=\Omega+\Lambda\left(\frac{x}{L}\right)+\Gamma\left(C\left(1-\frac{x}{L}\right)+1\right)^{-\beta/(1-\delta)}, \quad (21)$$

where

$$\Omega=1+\frac{1}{C}\left[\frac{1-\delta}{1-n}\right]\frac{1+C}{\frac{\epsilon_{s\,av}}{\phi_s}-1}, \qquad \Lambda=\frac{\beta/(1-n)}{\frac{\epsilon_{s\,av}}{\phi_s}-1},$$

and

$$\Gamma=-\frac{1}{C}\left[\frac{1-\delta}{1-n}\right]\frac{\left(1+\frac{\Delta P_c}{P_a}\right)^{1-n}}{\frac{\epsilon_{s\,av}}{\phi_s}-1}.$$

Notably, both Ω and $\Lambda > 0$, while $\Gamma < 0$. At $x = L$, Eq. 21 becomes

$$\frac{q_{R,i}}{q_1}=\Omega+\Lambda+\Gamma=1-\frac{\phi_s}{\epsilon_{s0}}\left[\frac{\epsilon_{s\,av}-\epsilon_{s0}}{\epsilon_{s\,av}-\phi_s}\right], \quad (22)$$

which corresponds to Eq. 35 in Tiller et al. (1999). At the $\phi_s \to \epsilon_{s0}$ limit, or when filtering a cakelike slurry, Eq. 22 becomes

$$\frac{q_{R,i}}{q_1}=0, \quad (23)$$

indicating that $u_s = u_L$ at cake surface.

On the other hand, at $x = 0$,

$$\frac{q_{R,i}}{q_1}=1. \quad (24)$$

Equation 24 is self-evident, as at the filter medium, $u_s = 0$ and $q_{R1} = q_{L1} = q_1$.

Equations 22–24 bind the two ends of the q_R-variation across the filter cake. Figure 2 depicts some q_R/q_1 curves according to the characteristic parameters listed in Table 1. Differentiation of Eq. 21 with respect to x/L leads to the following results:

$$\frac{d(q_R/q_1)}{d(x/L)}=\Lambda+\Gamma C\frac{\beta}{1-\delta}\left[C\left(1-\frac{x}{L}\right)+1\right]^{-\beta/(1-\delta)-1} \quad (25a)$$

and

$$\frac{d^2(q_R/q_1)}{d(x/L)^2}=-\frac{C\beta}{1-\delta}\frac{\left(1+\frac{\Delta P_c}{P_a}\right)^{1-n}}{\frac{\epsilon_{s\,av}}{\phi_s}-1}\times\left[C\left(1-\frac{x}{L}\right)+1\right]^{-\beta/(1-\delta)-2}. \quad (25b)$$

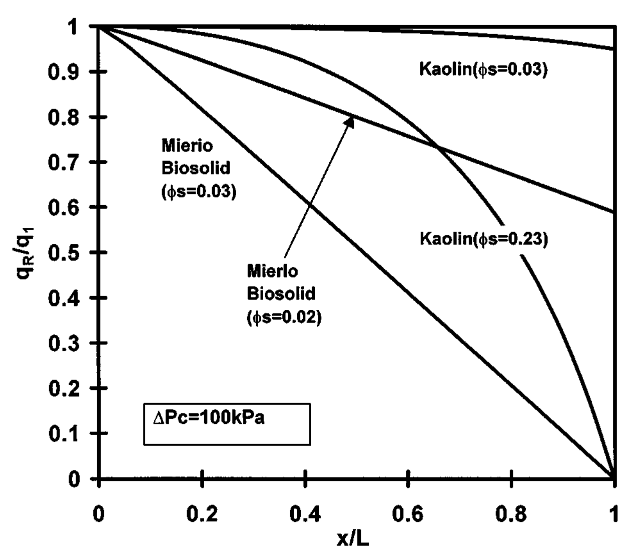

Figure 2. Relative flow-rate ratio for kaolin and Mierlo biosolid.

Table 1. Characteristic Parameters

Material	Kaolin*	Mierlo Biosolid**	Activated Sludge†	Water Treatment Plant Residue†
ϵ_{s0}	0.32	0.03	0.05	0.035
α_0, m^{-2}	2.88×10^{14}	4.02×10^{12}	3.62×10^{14}	7.93×10^{14}
k_0, m^2	1.09×10^{-14}	8.30×10^{-12}	5.53×10^{-14}	3.60×10^{-14}
β	0.09	0.47	0.26	0.22
n	0.55	1.83	1.40	1.03
δ	0.64	2.30	1.66	1.25
P_a, Pa	19,000	1,000	190	170

*Tiller and Horng (1983).
**La Heij (1994).
†Kwon (1995).

Equation 25a becomes zero only at $x=0$, the filter medium, and is negative elsewhere. In addition, Eq. 25b is always negative, indicating a concave-downward distribution for q_R. Therefore, neither a local maximum nor a local minimum of the q_R-variation exists over the entire cake except at the filter medium. Therefore, the extreme values of F_ω and F_x could be estimated according to the q_R values at the septum.

For a highly compactible filter cake where $n>1$ and $\delta>1$, Eq. 21 reduces to the following form since, in general, $\Delta P_c \gg P_a$:

$$\frac{q_R}{q_1}=1-\frac{\beta\phi_s}{\epsilon_{s0}(\delta-1)-\phi_s(n-1)}\left(\frac{x}{L}\right), \tag{26}$$

which denotes a straight line. When filtering a cakelike slurry, where $\epsilon_{s0}\to\phi_s$, Eq. 26 becomes

$$\frac{q_R}{q_1}=1-\left(\frac{x}{L}\right), \tag{27}$$

a straight line connecting (1,0) and (0,1) on the q_R/q_1 vs. x/L plot.

Substituting Eq. 21 into Eqs. 13a and 13b and then integrating with respect to x/L, yields

$$F_\omega=\frac{1}{\dfrac{\epsilon_{s\,\mathrm{av}}}{\phi_s}-1}\,\frac{\epsilon_{s0}}{C\epsilon_{s\,\mathrm{av}}}\left[\frac{1-\delta}{1-n}\right]$$
$$\cdot\left\{\begin{aligned}&1-\frac{\epsilon_{s\,\mathrm{av}}}{\phi_S}-\frac{\beta}{1-n}-\frac{1-\delta}{1-n}\,\frac{1+C}{C}-\left(\frac{1-\delta}{1-n}\right)\frac{\beta}{C(2-n-\delta)}\\&-\left[2-\frac{\epsilon_{s\,\mathrm{av}}}{\phi_S}-\frac{1-\delta}{1-n}\,\frac{1+C}{C}\right](1+C)^{(1-n)/(1-\delta)}+\frac{\beta}{C(2-n-\delta)}\,\frac{1-\delta}{1-n}(1+C)^{(2-n-\delta)/(1-\delta)}\end{aligned}\right\}, \tag{28}$$

and

$$F_x^{-1}=1+\frac{1}{\dfrac{\epsilon_{s\,\mathrm{av}}}{\phi_s}-1}\left[\frac{1-\delta}{1-n}\right]\left\{1+\frac{\beta}{2(1-\delta)}+\frac{1}{C}+\frac{1-\delta}{C^2(1-\beta-\delta)}\left[(1+C)^{(1-n)/(1-\delta)}-(1+C)^2\right]\right\}. \tag{29}$$

Notably, $F_\omega\le1$ and $F_x\ge1$.

For a highly compactible filter cake where $\delta>1$ and $n>1$, and with $\Delta P_c\gg P_a$, Eqs. 28 and 29 can be simplified as follows:

$$F_\omega=1+\frac{1}{\dfrac{\epsilon_{s0}(1-\delta)}{\phi_s(1-n)}-1}\left\{\frac{\beta}{2-n-\delta}\right\} \tag{30}$$

and

$$F_x^{-1}=1+\frac{1}{\dfrac{\epsilon_{s0}(1-\delta)}{\phi_s(1-n)}-1}\left\{\frac{\beta}{2(1-n)}\right\}. \tag{31}$$

At the $\phi_s\to\epsilon_{s0}$ limit, Eqs. 30 and 31 can be further reduced to

$$F_\omega=\frac{1-\delta}{2-n-\delta} \tag{32}$$

and

$$F_x^{-1}=\frac{1}{2}. \tag{33}$$

Restated, $1\le F_x\le2$. A heuristic rule states that one can approximately state $\delta=5n/4$. By allowing $\delta\to\infty$, Eq. 32 becomes

$$F_\omega=1/1.8=0.556. \tag{34}$$

Restated, $0.556\le F_\omega\le1$. Therefore, Eqs. 33 and 34 provide the upper bounds of deviations to estimate specific resistance and permeability while assuming constant-q_L.

Table 2 lists some sample calculations for highly compactible biosolids and moderately compactible kaolin slurry. For kaolin with a lower solid concentration, the deviation is relatively small (1%). However, as Table 2 implies, the deviation can exceed 28% for α_{av} and 41% for k_{av} when treating the kaolin slurry at a high solid concentration (32% v/v). For

Table 2. Calculated F_ω and F_x Values on the Basis of Eqs. 28 and 29

	F_ω	F_x
Kaolin:* $\phi_s = 0.03$	0.997	1.002
Kaolin:* $\phi_s = 0.32$	0.721	1.410
Mierlo biosolid:** $\phi_s = 0.02$	0.841	1.251
Mierlo biosolid:** $\phi_s = 0.03$	0.614	1.955
Activated sludge:† $\phi_s = 0.02$	0.930	1.097
Activated sludge:† $\phi_s = 0.05$	0.632	1.877
Water treatment plant residue: $\phi_s = 0.02$	0.897	1.167
Water treatment plant residue: $\phi_s = 0.035$	0.726	1.618

*Tiller and Horng (1983).
**La Heij (1994).
†Kwon (1995).

the biosolid from La Heij (1994), the corresponding deviations generally exceed those of kaolin slurry. Notably, the deviations listed in Table 2 are less than the upper bounds by Eqs. 33 and 34. In addition, our results suggest that in addition to the highly compactible biosolids, the moderately compactible kaolin could also have a marked error when estimating cake characteristics if its concentration is high.

Nonzero-u_s Case

In this section, we release the $u_s = 0$ restriction and, in doing so, derive the solution of the corresponding governing equation, Eq. 17. Double-integration of Eq. 17 with respect to X leads to the following close-form solution of $P(X)$:

$$\int_{1+\gamma P}^{1+\gamma} \frac{dy}{\dfrac{Q^*}{\beta} y^{\delta} - C_1 y^{\delta-\beta}} = X, \tag{35}$$

where C_1 is the integration constant and can be evaluated on the basis of the following integral:

$$\int_{1}^{1+\gamma} \frac{dy}{\dfrac{Q^*}{\beta} y^{\delta} - C_1 y^{\delta-\beta}} = 1. \tag{36}$$

The variable y in Eqs. 35 and 36 is defined as $1+\gamma P$. Notably, the derivations of Eqs. 35 and 36 are not based on the q_L-variation in Eq. 19.

Consider the slurry whose constitutive equations are available. Apparently, quantitatively evaluating Eqs. 35 and 36 requires the $q_1(t)$ and $L(t)$ data under the constant ΔP_c (γ-value). For example, at time t, the q_1 and L values are known. Then, the corresponding C_1 value at time t can be numerically evaluated according to Eq. 36. The P_s profile can be subsequently obtained by integrating Eq. 35.

The $q_1(t)$ and $L(t)$ data can be obtained by experiments or by simulations. For the latter approach, Stamakatis and Tien (1991) formulated the procedures that can numerically estimate the change in filtrate flow rate and cake thickness. However, among the many uncertainties include migration of fine particles within the pores of the filter cake (Tien et al., 1997) and sedimentation effects (Tiller et al., 1995) that cannot be easily incorporated into the model. Herein, we adopt the experimental data from Kwon (1995).

Figure 3 depicts the $q_1(t)$ data for two sludges from Kwon (1995), denoted as ‘‘activated sludge’’ (AS) and ‘‘wastewater treatment plant residue’’ (WT), respectively. Table 1 lists their rheological parameters. Both sludges are highly compactible since their n values all exceed unity (Tiller and Kwon, 1998). Furthermore, it is noteworthy that the two sludges exhibit very similar dewatering performance.

Figures 4a and 4b illustrate the time evolutions of the calculated solid pressure distributions across the cake on the basis of the experimental data from Kwon (1995). The uncertainties in these calculations are attributed to the possible errors inherent to the experimental q_1 and L data. Three points are worth mentioning. First, as time proceeds, the normalized solid pressure vs. x/L curve for both sludges shifts downward and leftward, indicating a compaction action of filter cake toward the filter medium. Restated, the distribution in P_s is not as curved at the start of the filtration. Second, the formation of the ‘‘skin layer’’ for these highly compactible sludges is apparent since the solid pressure decays to less than 10% of the total pressure drop as x/L exceeds 0.1. Third, all curves have converged to the ‘‘zero-u_s’’ case as $t > 100$ s, denoted as the curves with ‘‘> 100.’’ Restated, the effects of considering a nonzero solid velocity diminish at 100 s after the start of filtration. The total filtration time for the AS test is 7,800 s, while that for the WT is 1440 s. Consequently, the period of time in which the solid velocity must be considered occupies only 7% for the AS, and less than 1.5% for the WT.

Calculating the solid pressure distribution allows us to evaluate q_L (Eq. 8), solidosity (Eq. 10), q_R (Eq. 12), whence $\bar{q}_{R,\omega}$ and $\bar{q}_{R,x}$, F_ω and F_x. Restated, the F_ω and F_x can be estimated once the P_s-distributions were found. Figure 5 displays the calculated F_ω values for the AS and WT data depicted in Figures 4a and 4b. The F_ω values are initially close to unity, and then decrease rather rapidly to around 0.5 as $t > t_c$. (Notably, these calculation results are based on Kwon's experimental data. As mentioned earlier, the uncertainties in these calculations are attributed to the possible errors inherent to the experimental q_1 and L data. For example, at $t = 10$

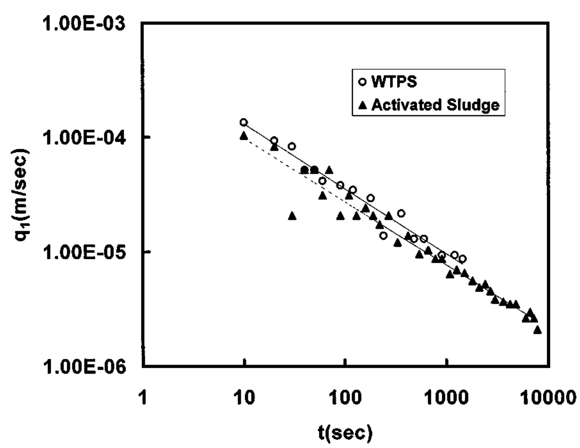

Figure 3. Variation of filtrate flow rate according to filtration time for highly compactible sludges.

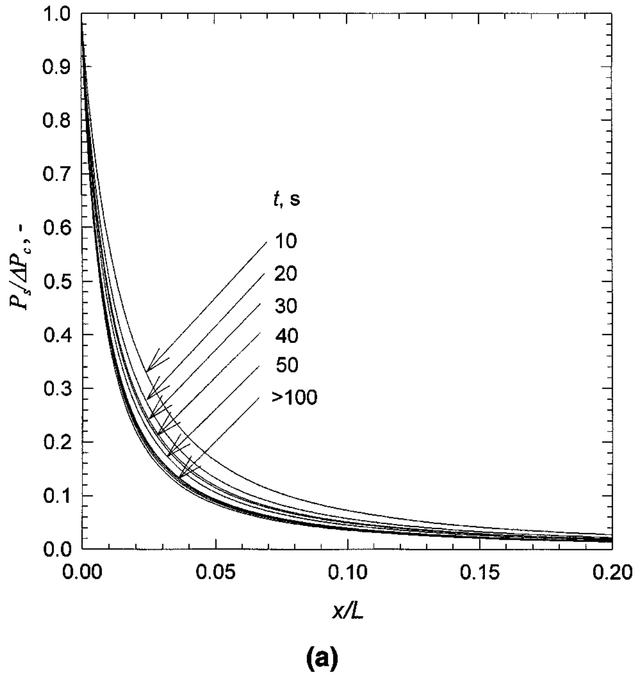

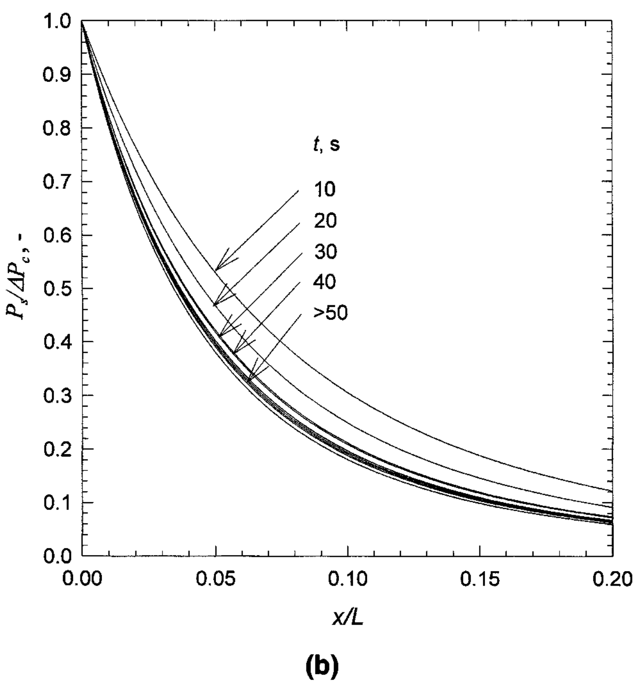

Figure 4. Solid pressure distributions across the cake on the basis of experimental data from Kwon (1995): (a) activated sludge; (b) wastewater treatment plant residue.

s, $F_\omega = 1.08$ rather than 1.0 for AS.) The critical time t_c is found close to 100 s, that is, consistent with the results in Figure 4. Such an observation is attributed to the relatively no-so-curved P_s- (whence the ϵ_S-) distribution at the beginning of the filtration when compared with those in the subsequent period of the test. The q_L-distribution can be evaluated on the basis of Eq. 3 as follows:

$$q_L - q_1 = \int_0^{x/L} \frac{x}{L} \frac{d\epsilon_s}{d(x/L)} \frac{dL}{dt} d\left(\frac{x}{L}\right). \tag{37}$$

Apparently, a less curved ϵ_s-distribution leads to a less curved q_L, thereby leading to a less curved q_R-distribution and a close-to-unity F_ω.

For an incompressible filter cake, the corresponding F_ω value is unity by definition. Interestingly, at the first phase of filtration, the behavior of a highly compactible filter cake resembles that of an incompressible cake. Furthermore, according to Figure 5, the F_ω value approaches 0.5 after $t > t_c$ for a highly compactible filter cake. Restated, the lower bound of F_ω (when considering the effects of nonzero solid velocity) is still bound by Eq. 32.

In summary, the zero-u approximation adopted by Tiller et al. (1999) is valid for interpreting filtration data of a highly compactible sludge cake except at the first stage of the filtration. Furthermore, the zero-u_s approach can be used to estimate the maximum error in cake characteristics when the solid velocity effect is not negligible.

Concluding Remarks

Conventional analysis used to interpret filtration data assumes a constant internal liquid flow rate (q_L) and a negligible solid velocity. When filtering a highly compactible filter cake, however, q_L definitely changes with the cake distance. In a pioneering work, Tiller et al. (1999) analyzed for the first time the variable-q_L in a compactible filter cake. Nevertheless, their approach is somewhat controversial, as it is based

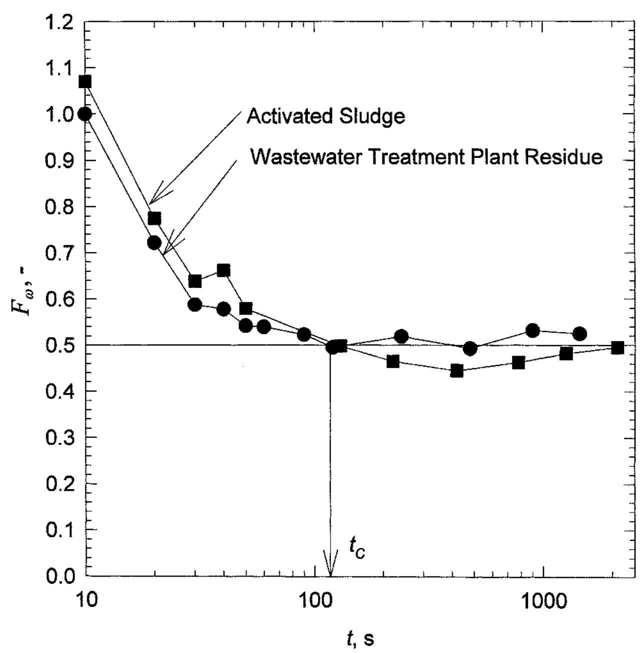

Figure 5. F_ω vs. t plot; the F_ω values are calculated on the basis of experimental data from Kwon (1995).

on the constant-q_L assumption. Furthermore, Tiller et al. did not derive the maximum errors that might be induced when estimating the cake characteristics on the basis of a constant-q_L approximation.

This work initially discussed the errors that might be generated when adopting a constant-q_L approximation for interpreting the filtration data. The upper bounds used for estimating a_{av} and k_{av} are also analytically derived. For a highly compactible filter cake, the maximum error induced sorely by adopting the constant-q_L assumption is 44% for α_{av} (F_ω) and 50% for k_{av} (F_x). Next, the effects of a nonzero solid velocity on the internal liquid flow rate are considered. The governing equation is analytically solved and a close-form solution is obtained as well. Two highly compactible sludges from Kwon (1995) are used in sample calculations. As time proceeds, the filter cake tends to be compacted toward the filter medium that forms a skin layer, and ultimately reaches the steady-state distribution predicted by the constant-q_L approximation as $t > 100$ s. The corresponding F_ω value is initially close to unity, indicating an "incompressible cakelike" behavior. It then decreases rather rapidly to that predicted by the constant-q_L approximation. As a result, except at the very first stage of the filtration, the approach by Tiller et al. (1999) is valid for interpreting filtration data of a highly compactible filter cake. Furthermore, the constant-q_L approximation provides the upper limit of possible error incurred when estimating cake characteristics regardless of the solid velocity effect.

Acknowledgments

National Science Council, ROC, financially supported this work.

Notation

b = fitting parameter, Pa^{-1}
$F_\omega = \alpha_{av}^c/\alpha_{av}$
$F_X = k_{av}^c/k_{av}$
k_0 = permeability at null stress, m^2
L = cake thickness, m
n = fitting parameter
P = dimensionless solid pressure
ΔP_C = pressure drop across the cake, Pa
Q^* = dimensionless parameter in Eq. 11
q_R = relative flow rate of liquid-to-solid phase, $m \cdot s^{-1}$
$q_{R,i}$ = relative flow rate of liquid-to-solid phase at cake surface, $m \cdot s^{-1}$
$\bar{q}_{R,\omega} = (1/\omega_c)\int_0^{\omega_c} q_R \, d\omega$
$\bar{q}_{R,x} = (1/L)\int_0^L q_R \, dx$
q_S = solid flow rate, $m \cdot s^{-1}$
q_i = liquid flow rate at cake surface, $m \cdot s^{-1}$
T = characteristic time, s
t_c = critical time, s
α_0 = local specific resistance of cake at null stress, $m \cdot kg^{-1}$
β = fitting parameter
Γ = dimensionless parameter in Eq. 21
Λ = dimensionless parameter in Eq. 21
ϵ_{s0} = solidosity at null stress
ϵ_{sav} = average solidosity
δ = fitting parameter
Ω = dimensionless parameter in Eq. 21
ω = variable indicating an arbitrary position in cake, m
ω_c = total solid volume in cake per unit sectional area, m

Literature Cited

Cleveland, T. G., F. M. Tiller, and J. B. Lee, "Theory of Filtration of Highly Compactible Biosolids," *Water Sci. Technol.*, **34**, 299 (1996).

He, D.-X., R. B. H. Tan, and C. Tien, "An Overview of Investigations on Filter Cake Characteristics," *Adv. Filter. Sep. Tech.*, **11**, 404 (1997a).

He, D.-X., R. B. H. Tan, and C. Tien, "An Investigation of the Filter Cake Characteristics in a Modified Compression-Permeability Cell," AIChE Meeting, Los Angeles, CA (1997b).

Jonsson, K. A., and B. T. L. Jonssen, "Fluid Flow in Compressible Porous Media: I. Steady-State Conditions," *AIChE J.*, **38**, 1340 (1992a).

Jonsson, K. A., and B. T. L. Jonssen, "Fluid Flow in Compressible Porous Media: II. Dynamic Behavior," *AIChE J.*, **38**, 1349 (1992b).

Kwon, J. H., "Effects of Compressibility and Cake Clogging on Sludge Dewatering Characteristics," PhD Diss., Seoul National Univ., Seoul, Korea (1995).

La Heij, E. J., "An Analysis of Sludge Filtration and Expression," PhD Diss., Technische Universiteit Eindhoven, Eindhoven, The Netherlands (1994).

Leu, W., "Principles of Compressible Cake Filtration," *Encyclopedia of Fluid Mechanics*, Vol. 5, N. P. Cheremisinoff, ed., Gulf Pub., Houston (1986).

Lu, W. M., F. M. Tiller, F. B. Chen, and C. T. Chien, "A New Method to Determine Local Porosity and Filtration Resistance of Filter Cakes," *J. Chin. Inst. Chem. Eng.*, **1**, 45 (1970).

Matsuda, A., K. Kawasaki, and M. Ishihara, "Compression-Permeability Characteristics and Effects of Freezing and Thawing Process of Excess Activated Sludges," *J. Chem. Eng. Jpn.*, **27**, 102 (1994).

Ruth, B. F., "Studies in Filtration: III. Derivation of General Filtration Equations," *Ind. Eng. Chem.*, **27**, 708 (1935).

Ruth, B. F., "Correlating Filtration Theory with Industrial Practice," *Ind. Eng. Chem.*, **38**, 564 (1946).

Ruth, B. F., G. H. Montillon, and R. E. Motonna, "Studies in Filtration: I. Critical Analysis of Filtration Theory," *Ind. Eng. Chem.*, **25**, 76 (1933a).

Ruth, B. F., G. H. Montillon, and R. E. Motonna, "Studies in Filtration: II. Fundamentals of Constant Pressure Filtration," *Ind. Eng. Chem.*, **25**, 153 (1933b).

Shirato, M. T., T. Aragaki, K. Ichimura, and N. Ootsuti, "Porosity Variation in Filter Cakes Under Constant Pressure Filtration," *J. Chem. Eng. Jpn.*, **4**, 172 (1970).

Shirato, M. T., T. Murase, H. Kato, and T. Aragaki, "Internal Flow Mechanism in Filter Cake," *AIChE J.*, **15**, 405 (1969).

Sorensen, P. B., and J. A. A. Hansen, "Extreme Compressibility in Biological Sludge Dewatering," *Water Sci. Technol.*, **28**, 133 (1993).

Sorensen, P. B., J. R. Christensen, and J. H. Bruus, "Effect of Small-Scale Solids Migration in Filter Cakes During Filtration of Waste-Water Solids Suspensions," *Water. Environ. Res.*, **67**, 25 (1995).

Sorensen, P. B., M. L. Agerbaek, and B. L. Sorensen, "Predicting Cake Filtration Using Specific Filtration Flow-Rate," *Water Environ. Res.*, **68**, 1151 (1996a).

Sorensen, P. B., P. Moldrup, and J. A. A. Hansen, "Filtration and Expression of Compressible Cakes," *Chem. Eng. Sci.*, **51**, 967 (1996b).

Sorensen, B. L., and P. B. Sorensen, "Structure Compression in Cake Filtration," *J. Environ. Eng. ASCE*, **123**, 345 (1997a).

Sorensen, B. L., and P. B. Sorensen, "Applying Cake Filtration Theory on Membrane Filtration Data," *Water Res.*, **31**, 665 (1997b).

Stamatakis, K., and C. Tien, "Cake Formation and Growth in Cake Filtration," *Chem. Eng. Sci.*, **46**, 1917 (1991).

Tien, C., R. Bai, and B. V. Ramarao, "Analysis of Cake Growth in Cake Filtration: Effect of Fine Particle Retention," *AIChE J.*, **43**, 33 (1997).

Tiller, F. M., "The Role of Porosity in Filtration: I. Numerical Methods for Constant Rate and Constant Pressure Filtration Based on Kozeny's Law," *Chem. Eng. Prog.*, **49**, 467 (1953).

Tiller, F. M., "The Role of Porosity in Filtration: II. Analytical Equations for Constant Rate Filtration," *Chem. Eng. Prog.*, **51**, 282 (1955).

Tiller, F. M., "The Role of Porosity in Filtration: III. Variable Pressure-Variable Rate Filtration," *AIChE J.*, **4**, 170 (1958).

Tiller, F. M., "Present Status of Filtration Theory," *Solid-Liquid Separation: A Review and Bibliography*, J. B. Poole and D. Doyle, eds., Her Majesty's Stationery Office, London, p. 13 (1966).

Tiller, F. M., and H. R. Cooper, "The Role of Porosity in Filtration: IV. Constant Pressure Filtration," *AIChE J.*, **6**, 595 (1960).

Tiller, F. M., and H. R. Cooper, "The Role of Porosity in Filtration: V. Porosity Variation in Filtration Cake," *AIChE J.*, **8**, 445 (1962).
Tiller, F. M., and T. C. Green, "The Role of Porosity in Filtration: IX. Skin Effect with Highly Compressible Materials," *AIChE J.*, **19**, 1266 (1973).
Tiller, F. M., and C. J. Huang, "Theory," *Ind. Eng. Chem.*, **53**, 529 (1961).
Tiller, F. M., and L. L. Horng, "Hydraulic Deliquoring of Compressible Filter Cakes, Reverse Flow in Filter Presses," *AIChE J.*, **29**, 297 (1983).
Tiller, F. M., and M. Shirato, "The Role of Porosity in Filtration: VI. New Definition of Filtration Resistance," *AIChE J.*, **10**, 61 (1964).
Tiller, F. M., and C. S. Yeh, "The Role of Porosity in Filtration: X. Deposition of Compressible Cakes on External Radial Surfaces," *AIChE J.*, **31**, 1241 (1985).
Tiller, F. M., and C. S. Yeh, "The Role of Porosity in Filtration: XI. Filtration Followed by Expression," *AIChE J.*, **33**, 1241 (1987).
Tiller, F. M., N. B. Hsyung, and D. Z. Cong, "The Role of Porosity in Filtration: XII. Filtration with Sedimentation," *AIChE J.*, **41**, 1153 (1995).
Tiller, F. M., and J. H. Kwon, "The Role of Porosity in Filtration: XIII. Unexpected Behavior of Highly Compactible Cakes," *AIChE J.*, **44**, 2159 (1998).
Tiller, F. M., R. Lu, J. H. Kwon, and D. J. Lee, "Variable Liquid Flow Rate in Compactible Filter Cakes," *Water Res.*, **33**, 15 (1999).
Wakeman, R. J., "Numerical Integration of the Differential Equations Describing the Formation of and Flow in Compressible Filter Cake," *Trans. Inst. Chem. Eng.*, **56**, 258 (1978).
Wakeman, R. J., "Thickening and Filtration: A Review and Evaluation of Recent Research," *Trans. Inst. Chem. Eng.*, **59**, 147 (1981a).
Wakeman, R. J., "The Formation and Properties of Apparently Incompressible Filter Cake on Downward Facing Surfaces," *Trans. Inst. Chem. Eng.*, **59**, 260 (1981b).
Wakeman, R. J., M. N. Sabri, and E. S. Tarleton, "Factors Affecting the Formation and Properties of Wet Compacts," *Powder Tech.*, **65**, 283 (1991).

Manuscript received Feb. 25, 1999, and revision received Aug. 5, 1999.